

## High-spin $E2$ bands in Kr isotopes

J. S. Clements, L. R. Medsker, L. H. Fry, Jr., and L. V. Theisen

Department of Physics, Florida State University, Tallahassee, Florida 32306

(Received 3 July 1979)

Bands of  $E2$  transitions are assigned to  $^{79}\text{Kr}$  and  $^{81}\text{Kr}$  on the basis of  $\gamma$ -ray singles,  $\gamma$ - $\gamma$  coincidence, angular distribution, and excitation function measurements. These bands can be interpreted as arising from the decoupling of  $g_{9/2}$  neutrons from the  $^{78}\text{Kr}$  and  $^{80}\text{Kr}$  cores, respectively, and a comparison is made with the previously reported  $^{77}\text{Kr}$  decoupled band. Relative reaction cross sections are in fair agreement with evaporation model calculations.

NUCLEAR REACTIONS  $^{72}\text{Ge}(^{10}\text{B}, x\gamma)$  and  $^{73}\text{Ge}(^{11}\text{B}, x\gamma)$ ,  $E=31, 34, 37, 40$  MeV; measured  $\sigma(E_\gamma, E)$ ,  $\sigma(E_\gamma, \theta)$ .  $^{73}\text{Ge}(^{11}\text{B}, x\gamma)$   $E=37$  MeV, measured Si(Li)-Ge(Li)  $\gamma$ - $\gamma$  coin.  $^{74,72}\text{Ge}(^{10}\text{B}, x\gamma)$   $E=40$  MeV; measured Ge(Li)-Ge(Li)  $\gamma$ - $\gamma$  coin.  $^{79,81}\text{Kr}$  deduced levels,  $J^\pi$ . Enriched targets.

### I. INTRODUCTION

Recent studies<sup>1,2</sup> have indicated that  $N=41$  nuclei are near the center of a deformed region in medium mass nuclei. In the low-mass region, studies<sup>3,4</sup> of the transitional nuclei  $^{72}\text{Se}$  and  $^{74}\text{Se}$  have explored shape coexistence suggested by the evidence for both rotational and vibrational states. The interacting-boson model<sup>5</sup> has been found to give an encouraging description of the data. A summary of the recent experimental and theoretical work can be found in Ref. 3. Calculations<sup>6</sup> in which particles are coupled to rotational cores have been applied to experimental results<sup>7,8</sup> for  $^{71,73}\text{As}$ ; however, the need for more work is indicated.

In the mass  $A=76-82$  region of deformed nuclei, few detailed experimental studies of the odd- $A$  transitional nuclei are found. Sequences of high-spin levels ( $\frac{9}{2}^+$ ,  $\frac{11}{2}^+$ ,  $\frac{13}{2}^+$ ,  $\frac{9}{2}^+$ ) have been observed<sup>9-12</sup> in  $^{79}\text{Rb}$ ,  $^{81}\text{Rb}$ ,  $^{77}\text{Br}$ , and  $^{77}\text{Kr}$ . These levels have transition energies resembling those of the ground state bands of the adjacent even-even cores and have been explained with the rotation aligned coupling model (RAC) of Stephens *et al.*<sup>13</sup>

The evidence for a decoupled band in  $^{77}\text{Kr}$  has been presented earlier.<sup>12</sup> In that work, the band of  $E2$  transitions built upon the  $\frac{9}{2}^+$  level was proposed on the basis of angular distribution and  $\gamma$ - $\gamma$  coincidence measurements. The present study was undertaken in order to identify further examples of this high-spin mode in other krypton isotopes.

### II. EXPERIMENTAL PROCEDURE

Beams of 30 to 40 MeV  $^{10}\text{B}$  and  $^{11}\text{B}$  were obtained from the Florida State University Super

FN Tandem Van de Graaff accelerator after extraction from the inverted sputter source.<sup>14</sup> Although more beam could be obtained, only 1-10 nA was required for these experiments. For the coincidence measurements,  $^{72,74}\text{Ge}$  targets were made by gluing milligram amounts onto Mylar backings. The targets were enriched to 96.4% and 94.5%, respectively. Reactions of boron on the constituents of the Mylar were determined by using Mylar targets. The relative reaction cross sections, excitation curves, and angular distributions were measured using  $\sim 1000 \mu\text{g}/\text{cm}^2$   $^{72}\text{Ge}$  or  $^{73}\text{Ge}$  evaporated onto thick Ta backings. The  $^{73}\text{Ge}$  enrichment was 78.4%.

The  $\gamma$  rays were measured on-line using Ge(Li) detectors with resolutions of  $\leq 2.8$  keV full width at half maximum (FWHM) at 1332 keV. Energy and efficiency calibrations were made using a calibrated NBS  $\gamma$ -ray source.<sup>15</sup> Low energy photons were observed with an 80 mm<sup>2</sup>  $\times$  5 mm Si(Li) detector. Focusing and collimation of the beam prior to bombardment of the target and the use of Ta target frames reduced the contamination of the  $\gamma$ -ray spectra. Measurements taken immediately after the beam was turned off were helpful for identifying reaction products. The  $\gamma$ - $\gamma$  coincidence measurements were made with two detectors at  $\pm 90^\circ$  to the beam, and the timing resolution was  $\sim 15$  nsec (FWHM). The data were accumulated and stored on magnetic tape by means of a Univac 6130 computer. Accurate values of  $\gamma$ -ray energies and intensities were obtained using a modified version of the program PEAKFIT.<sup>16</sup> This routine uses a Gaussian curve to fit the peaks, and the experimenter sets background shapes via an interactive scope. Our quoted uncertainties are based upon estimated statistical error and variations using alternative

fitting procedures and backgrounds. Previously well-known  $\gamma$  rays also produced in these reactions served as checks of the accuracy of our results.

The coincidence data were accumulated event by event and written on tape for off-line reduction. Using the code RAMPS,<sup>17</sup> we were able to sort on specific peaks or background regions of the Ge(Li) spectra and also on various parts of the TAC spectra. Final Ge(Li) coincidence spectra were corrected for background contributions by subtracting spectra generated by gating over continuum regions adjacent to the peaks. The accidental spectra were produced by gating over areas adjacent to the TAC peak.

The excitation functions were obtained for energies of 31, 34, 37, and 40 MeV using the evaporated  $^{72}\text{Ge}$  and  $^{73}\text{Ge}$  targets. The Ge(Li) detector was fixed at  $90^\circ$  to the beam, and the relative normalization was determined from the integrated beam charge at each bombarding energy. The angular distributions were obtained at angles of 40, 55, 70, and  $90^\circ$  with respect to the beam direction. Another Ge(Li) detector fixed at  $90^\circ$  on the other side of the beam line served as a monitor for an additional measure of the normalization.

### III. RESULTS

#### A. Reaction cross sections

The relative reaction cross sections were deduced for the  $^{10}\text{B} + ^{72}\text{Ge}$  and  $^{11}\text{B} + ^{73}\text{Ge}$  reactions at beam energies of 40 MeV. The transitions to the ground states of the various residual nuclei were taken as a measure of the reaction cross sections  $\sigma_R$ . Where necessary, corrections were made for feeding due to activities, internal conversion, and anisotropy of the  $\gamma$ -ray yields. Contributions due to possible unobserved ground state feedings are expected to be very weak because cascades through yrast states are dominant in  $(\text{HI}, x\gamma)$  reactions.

Evaporation model calculations of  $\sigma_R$  obtained with the code ALICE<sup>18</sup> are compared to the experimental  $\sigma_R$  in Fig. 1. The  $\sigma_R$  from ALICE were calculated at 39 MeV because of beam energy loss in the target and were normalized to the value of  $^{79}\text{Kr}$  in the  $^{10}\text{B} + ^{72}\text{Ge}$  reaction. In the  $^{11}\text{B} + ^{73}\text{Ge}$  reaction, the  $\sigma_R$  were normalized to the average of the values for  $^{81}\text{Kr}$ ,  $^{80}\text{Rb}$ ,  $^{80}\text{Kr}$ , and  $^{78}\text{Br}$ . For the  $^{73}\text{Ge} + ^{11}\text{B}$  reaction, ALICE calculations are consistent with the yields for the  $p2n$ ,  $p3n$ ,  $4n$ , and  $\alpha2n$  products. However, ALICE greatly underpredicts the  $3n$  channel and predicts population of the  $\alpha3n$  product, which was not observed. As can be seen in the figure, three- and four-particle emission dominates.

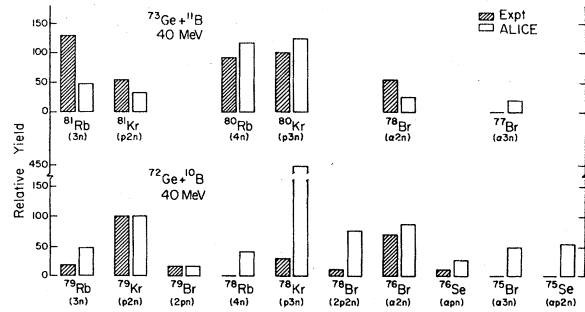


FIG. 1. Experimental relative reaction cross sections compared to those predicted by ALICE, for the  $^{11}\text{B} + ^{73}\text{Ge}$  and  $^{10}\text{B} + ^{72}\text{Ge}$  reactions.

For the  $^{72}\text{Ge} + ^{10}\text{Be}$  reaction, ALICE predictions compare favorably with the measured yields of the  $p2n$ ,  $2pn$ , and  $\alpha2n$  products. However, ALICE grossly overpredicts the  $p3n$  channel and predicts population of the  $4n$ ,  $\alpha3n$ , and  $\alpha p2n$  channels, which are not observed. Three-particle

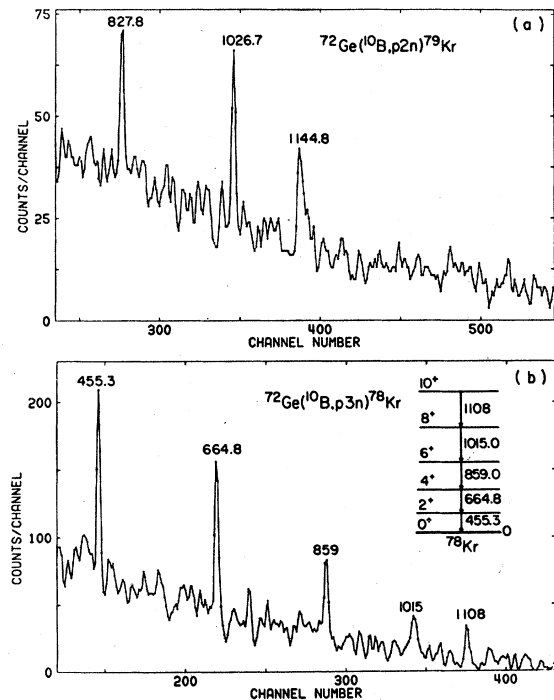


FIG. 2. Coincidence results: (a) Ge(Li)-Ge(Li)  $\gamma$ - $\gamma$  coincidence results for  $^{72}\text{Ge}(^{10}\text{B}, p2n)^{79}\text{Kr}$  at 38 MeV. This spectrum is the sum of the background-subtracted spectra generated by gates on the 827.8-, 1026.7-, and 1144.8-keV  $\gamma$  rays. The individual gated spectrum each contain the other members of the proposed band in  $^{79}\text{Kr}$ . (b) Coincidence results for the  $^{72}\text{Ge}(^{10}\text{B}, p2n)^{78}\text{Kr}$  reaction at 37 MeV. This background-subtracted spectrum is the sum of those generated by gates on the 664.8-, 859.0-, and 1015.0-keV  $\gamma$  rays.

TABLE I. Energies of  $\gamma$  rays which have been assigned to E2 bands in  $^{78}\text{Kr}$ ,  $^{79}\text{Kr}$ , and  $^{81}\text{Kr}$ .

$^{78}\text{Kr}$		$^{79}\text{Kr}$		$^{81}\text{Kr}$
Present work	Ref. 19	Present work	Ref. 22	Present work
455.3 $\pm$ 0.5	455.3 $\pm$ 0.8	827.8 $\pm$ 0.5	826.6 $\pm$ ?	926.6 $\pm$ 0.5
664.8 $\pm$ 0.5	664.7 $\pm$ 1.0	1026.7 $\pm$ 0.5		1158.5 $\pm$ 0.8
859.0 $\pm$ 0.7	858 $\pm$ 1.5	1144.8 $\pm$ 1.0		1257 $\pm$ 1
1015.0 $\pm$ 0.5	1015 $\pm$ 1.5			
1108 $\pm$ 1	1110 $\pm$ 1.5			

emission dominates for this reaction with more proton channels involved. This is a result of the compound nucleus being more neutron deficient. In the even-even products  $^{78}\text{Kr}$  and  $^{76}\text{Se}$ , the ground state rotational bands are strongly populated, as can be seen for  $^{78}\text{Kr}$  in Fig. 2(b) and Table I.

#### B. Level scheme of $^{79}\text{Kr}$

The nucleus  $^{79}\text{Kr}$  has a ground state spin<sup>20,21</sup> and parity of  $\frac{1}{2}^-$ . Recent measurements of the  $\beta^+$  decay of  $^{79}\text{Rb}$  by Lipták and Kristiak<sup>21</sup> show a low-lying  $\frac{9}{2}^+$  level at 148.82 keV which is depopulated only by a 19.1-keV  $\gamma$  ray to the isomeric  $\frac{7}{2}^+$  state at 129.72 keV.

In the present work, we used the reaction

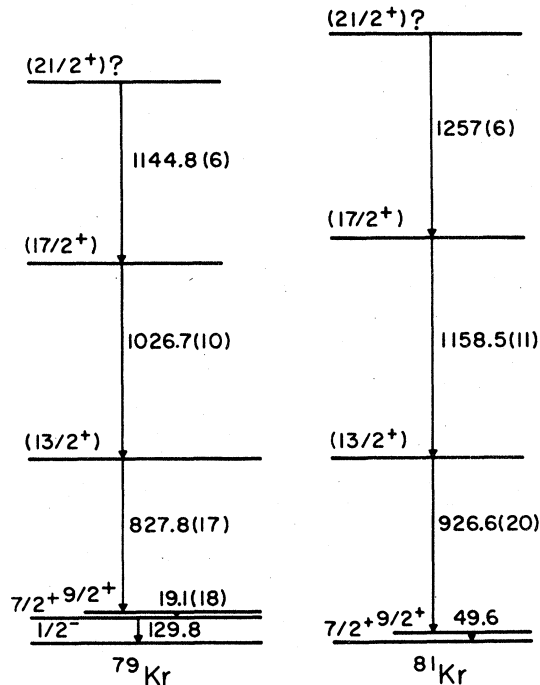


FIG. 3. Proposed positive-parity bands in  $^{79}\text{Kr}$  and  $^{81}\text{Kr}$ . The  $\gamma$ -ray relative intensities are in parentheses.

$^{72}\text{Ge}(^{10}\text{B}, p2n\gamma)$  to study  $^{79}\text{Kr}$ . Using information from  $\text{Ge}(\text{Li})\text{-Ge}(\text{Li})$   $\gamma$ - $\gamma$  coincidence, angular distribution, excitation function, and intensity measurements, a high-spin band of E2 transitions (shown in Fig. 3) was constructed from three  $\gamma$  rays with energies of 827.8, 1026.7, and 1144.8 keV (see Table I). The coincidence spectrum is shown in Fig. 2(a). The angular distributions for the 827.8- and 1026.7-keV  $\gamma$  rays each have the characteristic shape expected for E2 transitions. The values of  $A_2/A_0$  and  $A_4/A_0$ , from fitting the data with  $W(\theta) = \sum A_n P_n(\cos\theta)$ , are given in Table II. Interference from other  $\gamma$  rays and weak yield precluded the measurement of an angular distribution for the 1144.8-keV  $\gamma$  ray. The excitation function of the 1026.7-keV  $\gamma$  ray, relative to the 827.8-keV  $\gamma$  ray is shown in Fig. 4. The larger slope for the 1026.7-keV  $\gamma$  ray is consistent with a placement in the level scheme in which states of sequentially lower spins are being deexcited. As can be seen in Fig. 3, the relative intensities of the  $\gamma$  rays are consistent with their placement in the level scheme. Due to the agreement of the intensities of the 19.1- and 827.8-keV  $\gamma$  rays, we propose that the band feeds the  $\frac{9}{2}^+$  level analogous to the band in  $^{81}\text{Kr}$ . This is in disagreement with the proposal of Anderson *et al.* (see Ref. 22) that the 827.8-keV  $\gamma$  ray feeds the  $\frac{7}{2}^+$  level. However, their assignment was tentative and was made before the  $\frac{9}{2}^+$  level was found.<sup>21</sup> Therefore we propose that the spins and parities of the levels in the band are  $\frac{9}{2}^+$ ,  $\frac{13}{2}^+$ , and  $\frac{17}{2}^+$ , with a  $J^\pi = \frac{21}{2}^+$  level likely.

TABLE II. Results of present angular distribution measurements for  $^{72}\text{Ge}(^{10}\text{B}, p2n)^{79}\text{Kr}$  at  $E_L = 40$  MeV and  $^{73}\text{Ge}(^{11}\text{B}, p2n)^{81}\text{Kr}$  at  $E_L = 37$  MeV.

Nucleus	Energy	$A_2/A_0$	$A_4/A_0$
$^{81}\text{Kr}$	926.6	0.30 $\pm$ 0.17	-0.21 $\pm$ 0.20
	1158.5	0.29 $\pm$ 0.07	-0.12 $\pm$ 0.09
$^{79}\text{Kr}$	827.8	0.26 $\pm$ 0.10	-0.09 $\pm$ 0.10
	1026.7	0.12 $\pm$ 0.13	-0.10 $\pm$ 0.13

C. Level scheme of  $^{81}\text{Kr}$ 

The nucleus  $^{81}\text{Kr}$  has a ground state spin and parity<sup>23</sup> of  $\frac{7}{2}^+$ . A low-lying  $\frac{9}{2}^+$  level was observed by Wilson *et al.*<sup>24</sup> at 49.6 keV using the  $^{81}\text{Br}(p, n\gamma)$  reaction.

In the present work, we have produced  $^{81}\text{Kr}$  via the compound nucleus  $^{84}\text{Kr}$  using the reactions  $^{73}\text{Ge}(^{11}\text{B}, 3n\gamma)$  and  $^{74}\text{Ge}(^{10}\text{B}, 3n\gamma)$ . A high-spin band (shown in Fig. 3) was constructed from measurements of Si(Li)-Ge(Li)  $\gamma$ - $\gamma$  coincidences, Ge(Li)-Ge(Li)  $\gamma$ - $\gamma$  coincidences, angular distributions, excitation functions, and intensities. Three  $\gamma$  rays with energies of 926.8, 1158.5, and 1257 keV (see Table I) were found to be in coincidence with each other and the 49.6-keV  $\gamma$  ray, which de-excites the  $\frac{9}{2}^+$  level. The angular distributions for the 926.6- and 1158.5-keV  $\gamma$  rays each have the characteristic shape expected for  $E2$  transitions, and the coefficients are shown in Table II. Since the band feeds the  $\frac{9}{2}^+$  level, we propose that the spins and parities of the levels in the band are  $\frac{9}{2}^+$ ,  $\frac{13}{2}^+$ , and  $\frac{17}{2}^+$ . The excitation functions (Fig. 4) and relative intensities (Fig. 3) of the  $\gamma$  rays are consistent with their placement in the proposed level scheme.

## IV. DISCUSSION

The known high-spin positive-parity levels in Kr isotopes are given in Fig. 5. The level spac-

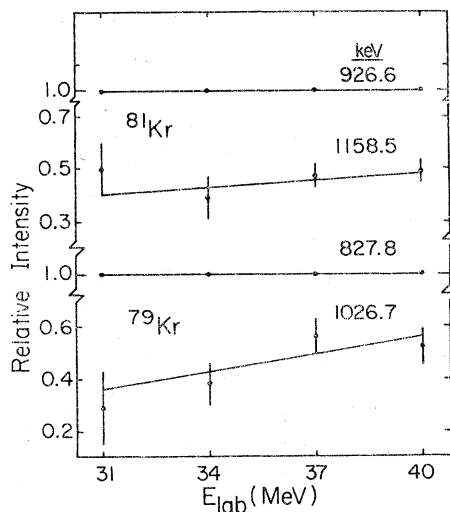


FIG. 4. Intensities of the 1158.5-keV  $\gamma$  ray relative to that of the 926.6-keV  $\gamma$  ray, and of the 1026.7-keV  $\gamma$  ray relative to that of the 827.8 keV  $\gamma$  ray, as a function of the projectile energy.

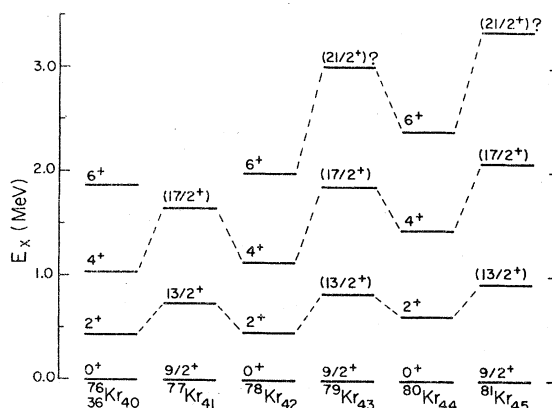


FIG. 5. Systematics of high-spin levels in krypton. The positive-parity bands in the odd- $A$  isotopes are shown in comparison with the ground state bands in the neighboring even-even isotopes. For ease of comparison, the energies of the odd- $A$  states have been shifted so that the  $\frac{9}{2}^+$  states line up with the  $0^+$  ground states. The data for  $^{76,77,78,80}\text{Kr}$  come from Refs. 25, 12, 9, and 26, respectively.

ings show a systematic increase as neutrons are added to the  $N=40$   $^{76}\text{Kr}$  nucleus. The even-even Kr isotopes have the characteristic ground state rotational bands ( $0^+$ ,  $2^+$ ,  $4^+$ ,  $6^+$ , ...). The resemblance of the bands in the odd- $A$  Kr's and the smooth trend as a function of  $N$  suggests a common theoretical interpretation.

The positive-parity levels in  $^{77}\text{Kr}$  have been discussed<sup>12</sup> in terms of the rotation-aligned coupling (RAC) model.<sup>13</sup> In this model, the odd particle is decoupled from the core by the Coriolis force, producing level spacings in the odd- $A$  nucleus which are similar to those of the core. One would also expect that the odd- $A$   $B(E2)$  values would be close to the ones for the corresponding transitions of the core.

Although the levels of the Kr isotopes are suggestive of decoupling, an interesting feature is the significantly higher energies of the odd- $A$  levels compared to those in the core. The same effect has been observed in the Se isotopes.<sup>27,28</sup> The softness of these nuclei allows the odd nucleon to disturb the simple relationship between the core and the core+particle systems. Thus, the explanation of the positive-parity levels requires more complicated calculations. The assumptions of a triaxial core and variable moment of inertia have yielded better results<sup>6,29</sup> in the RAC calculations for other nuclei in this mass region. Alternatively, particle-vibrational coupling calculations developed by Alaga and Paar<sup>30</sup> have given equally encouraging results.

The differences in the Kr odd- $A$  and even- $A$  level energies suggest a situation similar to the Se nuclei, although more experimental and theoretical work is needed. To that end, it would be good to have measurements of  $B(E2)$  values and spectroscopic strengths for the Kr levels, including the unfavored levels.

## ACKNOWLEDGMENTS

We thank Bob Leonard for preparing the targets. The help of L. A. Parks with the data acquisition and R. V. LeClaire with the data reduction is appreciated. Our work was supported in part by the National Science Foundation.

- 
- <sup>1</sup>M. N. Vergnes *et al.*, Phys. Lett. 72B, 447 (1977).  
<sup>2</sup>J. F. Mateja *et al.*, Phys. Rev. C 17, 2047 (1978).  
<sup>3</sup>K. P. Lieb and J. J. Kolata, Phys. Rev. C 15, 939 (1977) and references therein.  
<sup>4</sup>A. V. Ramagya *et al.*, Phys. Rev. C 12, 1360 (1975) and references therein.  
<sup>5</sup>A. Arima and F. Iachello, Phys. Rev. Lett. 35, 1069 (1975).  
<sup>6</sup>H. Toki and A. Faessler, Phys. Lett. 63B, 121 (1976).  
<sup>7</sup>C. Protop *et al.*, Z. Phys. 271, 65 (1974).  
<sup>8</sup>B. Heits *et al.*, Phys. Rev. C 15, 1742 (1977).  
<sup>9</sup>J. S. Clements *et al.*, Phys. Rev. C 20, 164 (1979).  
<sup>10</sup>H. G. Friedericks *et al.*, Phys. Rev. C 13, 2247 (1976).  
<sup>11</sup>M. A. Deleplanque *et al.*, J. Phys. Lett. 35, L-237 (1974).  
<sup>12</sup>E. Nolte and P. Vogt, Z. Phys. A275, 33 (1975).  
<sup>13</sup>F. S. Stephens, R. M. Diamond, and S. D. Nilsson, Phys. Lett. 44B, 429 (1973).  
<sup>14</sup>K. R. Chapman, Nucl. Instrum. Methods 124, 229 (1975).  
<sup>15</sup>Mixed radionuclide standard (4215E) from the National Bureau of Standards.  
<sup>16</sup>The code PEAKFIT courtesy of P. P. Singh, Indiana University Cyclotron Facility. Modified by R. V. LeClaire for interactive scope use at Florida State University.  
<sup>17</sup>The Code RAMPS, written by R. V. LeClaire, Florida State University (unpublished).  
<sup>18</sup>The code OVERLAID ALICE was supplied courtesy of M. Blann, University of Rochester. The code is described in NSRL Report No. COO-3494-34, 1977..  
<sup>19</sup>P. P. Urone and F. E. Bertrand, Nucl. Data Sheets 15, 107 (1975).  
<sup>20</sup>P. P. Urone and D. C. Kocher, Nucl. Data Sheets 15, 257 (1975).  
<sup>21</sup>J. Liptak and J. Kristiak, Nucl. Phys. A311, 421 (1978).  
<sup>22</sup>P. P. Urone and D. C. Kocher, Nucl. Data Sheets 15, 257 (1975).  
<sup>23</sup>J. F. Lemming, Nucl. Data Sheets 15, 137 (1975).  
<sup>24</sup>D. C. Wilson *et al.*, Phys. Rev. C 16, 2070 (1977).  
<sup>25</sup>F. E. Bertrand and R. L. Auble, Nucl. Data Sheets 19, 507 (1976).  
<sup>26</sup>L. R. Greenwood, Nucl. Data Sheets 15, 289 (1975).  
<sup>27</sup>P. von Brentano, B. Heits, and C. Protop, in *Prob- lems of Vibrational Nuclei*, edited by G. Alaga, L. Sips, and V. Paar (North-Holland, Amsterdam, 1975), p. 155.  
<sup>28</sup>K. O. Zell *et al.*, Z. Phys. A272, 27 (1975).  
<sup>29</sup>H. P. Hellmeister *et al.*, Phys. Rev. C 17, 2113 (1978).  
<sup>30</sup>G. Alaga and V. Paar, Phys. Lett. 61B, 129 (1976).